Available online at www.sciencedirect.com
ScienceDirect
Optics Communications 266 (2006) 592–597
OPTICS COMMUNICATIONS
www.elsevier.com/locate/optcom

Dual-band multiplexer/demultiplexer with photonic-crystal-waveguide couplers for bidirectional communications

Forest Shih-Sen Chien [a], Sue-Cheng Cheng [b], Yu-Ju Hsu [c,d], Wen-Feng Hsieh [c,*]

[a] *Department of Physics, Tunghai University, Taichung, Taiwan*
[b] *Department of Physics, Chinese Culture University, Taipei, Taiwan*
[c] *Department of Photonics Engineering and Institute of Electro-Optical Engineering, National Chiao Tung Univeristy, Ta-Hsueh Road 1001, Hsinchu 30050, Taiwan*
[d] *Innolux Display Corp., Mauli, Taiwan*

Received 17 December 2005; received in revised form 24 May 2006; accepted 26 May 2006

Abstract

An ultrashort photonic-crystal-waveguide (PCW) coupler is numerically designed for dual-band multiplexing/demultiplexing (Muxing/Demuxing). The PCW coupler consists of two line defects of reduced rods in a triangular lattice and Muxing/Demuxing is implemented by the distinction between coupling and decoupling of PCWs. Since waves tend to highly localize within the reduced rods, the backward coupling is suppressed and the efficiency of Muxing/Demuxing is enhanced as compared with the void-rod PCWs. The coupler is utilized to build a bidirectional system for dual-band duplex communications.

Keywords: Photonic crystal waveguides; Decoupling; Multiplexing/demultiplexing; Bidirectional communication

1. Introduction

The dual-band multiplexer/demultiplexer (Muxer/Demuxer) is a key component for bidirectional data traffics [1,2] applied for optical communication from the wide area networks to the local area networks. One simple and useful application, for example, is a duplex communication over a single fiber, where the data capacity is doubled without installing a new fiber. Up to date, the dual-band Muxer/Demuxer is implemented with conventional optical components, e.g., multiple layer thin film filters, gratings, and optical couplers. The components are at the millimeter scale and technical-intensively assembled by hands. As the data capacity at the user ends dramatically increases (such as the fiber-to-the-home application), there is a strong demand for mass production and high integration of the components of the duplexers.

Line defects in a photonic crystal (PhC) can be utilized as waveguides of electromagnetic (EM) waves, the so-called photonic crystal waveguides (PCWs) [3]. The guiding mechanism is attributed to the bandgap confinement. PCWs surpass conventional waveguides with many unique features, e.g., low group velocity [4], large dispersion [5], and low transmission loss through sharp bends [6], offering a potential approach to design and produce large-scale miniaturized photonic integrated circuits (PICs). The coupling of two PCWs gives rise to the splitting of the dispersion of their guided modes. It is analogue to symmetrical double potential wells in quantum mechanics where the supermode, superposition of the symmetric and anti-symmetric eigenmodes, oscillates between the wells.

Couplers are one of the most promising elements of PCWs as building blocks for PICs [7–9]. Variety of functional devices based on PCW couplers have been proposed recently, e.g., featuring switches [10,11], channel-drop filter

* Corresponding author. Tel.: +886 3 5712121x56316; fax: +886 3 5716631.
E-mail address: wfhsieh@mail.nctu.edu.tw (W.-F. Hsieh).

0030-4018/$ - see front matter © 2006 Elsevier B.V. All rights reserved.
doi:10.1016/j.optcom.2006.05.055

[12], power splitter [13], and wavelength Muxer and Demuxer [9,14,15], etc., representing the potential prospective of PCW couplers for photonic applications. We have proposed that an ultrashort dual-band Demuxer with void-rod (defects introduced by removal of rods) PCWs can be designed by the distinction between coupling and decoupling [16]. Decoupling occurs with two parallel PCWs in triangular-lattice PhC (note that in square-lattice PhC, decoupling only occurs with void-rod PCWs when there are an odd number of rows between waveguides [17]). However, a backward coupling exists in the Demuxer, giving rise to the degradation of its performance. To overcome this issue, a PCW coupler with a loop-shape arm is proposed. The Demuxing efficiency reaches the maximum as two branches of waves are in phase at the merging point in the loop. The discrete spacing of the PCWs imposes constrains to the design of the loop-shape arm and increases the difficulty. In addition, the loop-shape design cannot implement a Muxer, because the coupling efficiency is poor as the wave is injected oppositely into the loop-shape arm.

Recently, it has been demonstrated numerically that the properties of PCW and the coupler can be varied by tuning the radius of the partition rods or the defect rods. The coupling coefficient of a PhC coupler can be increased as the radius of the partition rods is reduced [7]. This feature can be applied to build ultrasmall channel interleavers and Demuxer. On the other hand, the coupling efficiency of PCWs with external lightwave circuits can be greatly improved as the PCWs consists of reduced-rod defects, since the stationary energy of EM waves in these PCWs will tend to localize in the reduced-rod defect [18]. We employ this concept of the EM wave localization to relieve the issue of the backward coupling in the PCW couplers. In this article, we discuss the cause of backward coupling in terms of energy flow in the PCWs. The energy flow is strongly perturbed by rods at the boundaries of the coupled PCWs. As a result, it is a ''turbulent'' flow rather than a ''laminar'' one and the backward scattering occurs. The situation is greatly improved as the reduced-rod defects substitute for the void-rod defects, because the energy is highly concentrated within the reduced rods. Consequently, the backward coupling is significantly suppressed regardless of the propagating direction. We numerically demonstrate a dual-band PCW Muxer/Demuxer with reduced-rod defects and propose a duplexer for bidirectional optical communication that is applicable to miniaturize PICs.

2. Energy distribution in PCWs

The PCW is not an index-homogeneous device due to its intrinsic periodic dielectrics; instead, the PCW can be considered as a sort of grating-assisted waveguide. The EM wave strongly interacts with wavelength-scale dielectrics, so it propagates in a manner different from a laminar flow. We consider the PhC composed of a triangular-lattice dielectric rods, where the lattice constant is Λ, and the radius and the dielectric constant of the rods are 0.2Λ and 12. The PCW is formed by removing a row of rods (i.e., void rods). We derive the electric-energy-density (U_e), equal to dielectric constant $\times$ electric eigenfield square, of guided modes at $k_x = 0.35$, i.e., $f = 0.43$, where k_x is the normalized wavevector with unit of $2\pi/\Lambda$ and f is the normalized frequency with unit of c/Λ in a PCW (Fig. 1(a)) by the plane wave expansion (PWE) method [19]. The U_e is normalized, as its integral over the computational cell is unit. The Poynting vectors tend to form energy vortices (the inset in Fig. 1(a)) around the rods along the PCW boundary [20]. The vortex becomes more significant as the wavevector gets closer to the zone boundary ($k_x = 0.5$). The energy concentrates at the rods along the boundary, because of the presence of the vortices. Accordingly, the U_e pattern of two coupled PCWs (Fig. 1(b)) also shows an essential amount of energy concentrated at the partition rods between the PCWs. Therefore, the energy flow is scattered while crossing the partition rods, accounting for the backward coupling.

We address the issue of the backward coupling in terms of the energy distribution. As the energy concentrated in the partition rods accounts for the scattering, the backward coupling should be reduced as the energy concentration in the partition rods is removed. To do so, we appeal to the decrease of the radius of defect rods; namely the defect is introduced by reducing the rod radius. Here, we consider the defect rod with a radius (R_d) of 0.1Λ (i.e., reduced rods). The U_e of a single PCW and the coupled PCWs with reduced-rod defects at $k_x = 0.4$ are shown in Figs. 2(a) and (b), and the inset in Fig. 2(a) shows the Poynting vectors of the single PCW near a reduced rod. Although, a rather little difference in effective refractive indices exists between the reduced rods and the void rods, the patterns of energy densities and Poynting vectors differ significantly. The energy tends to be highly localized in the reduced rods. For the coupled PCWs separated by one row of rods, the energy density is still mainly localized at the reduced rods.

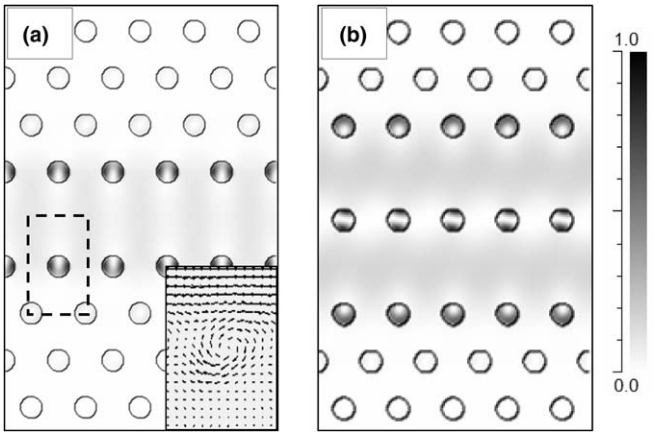

Fig. 1. Electric energy densities (U_e) of a void-rod PCW (a) and coupled PCWs (b) in a 2D PhC. The inset in (a) is the pattern of Poynting vectors near a rod at the boundary marked by the dashed line.

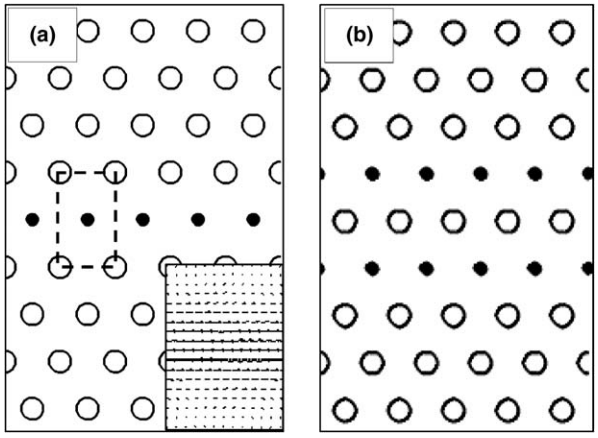

Fig. 2. U_e of a reduced-rod PCW (a) and coupled PCWs (b). The inset in (a) is the pattern of Poynting vectors near the reduced rod marked by the dashed line.

From the pattern of Poynting vectors, the energy flow is laminar in the reduced-rod PCW with no energy vortices.

Fig. 3 shows the remarkable contrast between electric energy densities along the centers of PCWs, where the ratio of the energy density peaks is 120, i.e., the ratio of square of field amplitude is amplified 10×, since the dielectric constant = 12. In a void-rod PCW, the modulation amplitude of energy is only 30%. However, in a reduced-rod PCW the peak value of U_e in the reduced rods is two orders of magnitude higher than the valley value in the air region. Almost 50% of energy concentrates within the reduced rods, although the rods take only 5% of area of one unit cell. Hence, the void-rod PCW can be considered as the superposition of a perfect PhC and a line of effectively "negative-dielectric-constant" rods. The EM wave is much less localized at the defect sites, where "negative-dielectric-constant" rod presents. On the other hand, the reduced rod still is a proper potential well, where the EM wave can be localized. Despite the reduced rod is smaller than one quarter of the wavelength, the energy still can be localized there. The scattering by the partition rods is proportioned to the overlap integral of field intensity times the difference of dielectric constants at the boundary of the rods. The scattering by the partition rods is suppressed, because the field intensity at the partition rods is dramatically reduced (see Section 3). In addition, the energy hopping between the reduced rods leads to a temporally transient scattering. Both factors account for the suppression of backward coupling. As the scattering is not significant, the grating-assisted nature of the coupler becomes negligible.

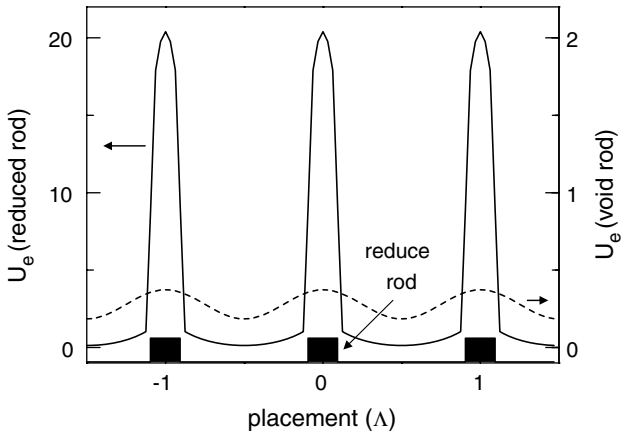

Fig. 3. Energy densities (U_e) along the centers of a void-rod PCW (Fig. 1(a)) and a reduced-rod PCW (Fig. 2(a)) at $k_x = 0.4$.

3. Coupling between reduced-rod PCWs

Two dispersion curves of the guided modes propagating in the coupled PCWs are generated due to the overlapping of the mode functions. The dispersion curves of two coupled reduced-rod PCWs with E-polarization, where the electric field is parallel to the dielectric rods, shown in Fig. 4(a) are derived by PWE. From the electric fields of the guided modes, we can identify that the fields appear as even parity at the points E_1 and E_2, and as odd parity at the points O_1 and O_2 (Fig. 4(b)). The situation is identical to that of void-rod PCWs, since the change of the defect radius cause the vertical shift to the dispersion curves. The dispersion curves cross each other and the frequency at the crossing point (denoted as f_d) is 0.363, corresponding to $k_x = 0.378$. The fundamental guided mode (referred to the mode with lowest frequency at $k_x = 0$) has odd parity. That conflicts with the conventional optical waveguide, in which fundamental guided modes are always even. Such an unusual situation can be accounted by the coupling of defects between two PCWs [21].

The even and odd guided modes propagate at different wavevectors, k_e and k_o, respectively. The superposition of these modes gives rise to beating that the energy would transfer periodically along two coupled PCWs. The coupling length L, defined as the propagation distance for a complete energy transferring, can be expressed as

$$L = \Lambda/(2 \cdot \Delta k), \tag{1}$$

where Δk is the absolute value of $(k_e - k_o)$ and is dispersive.

We plot L and Δk *vs.* frequency f in Fig. 5(a) using Eq. (1), where Δk is obtained from dispersion curves. The Δk vanishes and L soars to infinity at f_d. Thus the eigenwaves propagate with equal wavevector ($k_e = k_o$ or $\Delta k = 0$) and the coupling length is infinite, implying no beating (i.e., no energy transferring) between the coupled PCWs. The coupler is "decoupled" as it is operated at f_d. Decoupling, a special feature offered by the coupled PCWs [9,16], leads to elimination of crosstalk between waveguides. Closely packed circuits can be built based on the concept of decoupling.

The other frequency $f_c = 0.314$ has $\Delta k = 0.1448$ with corresponding L of 3.45Λ. We verify the predicted L by simulating the real time evolution of the EM wave traveling through the coupled PCWs by the finite-difference

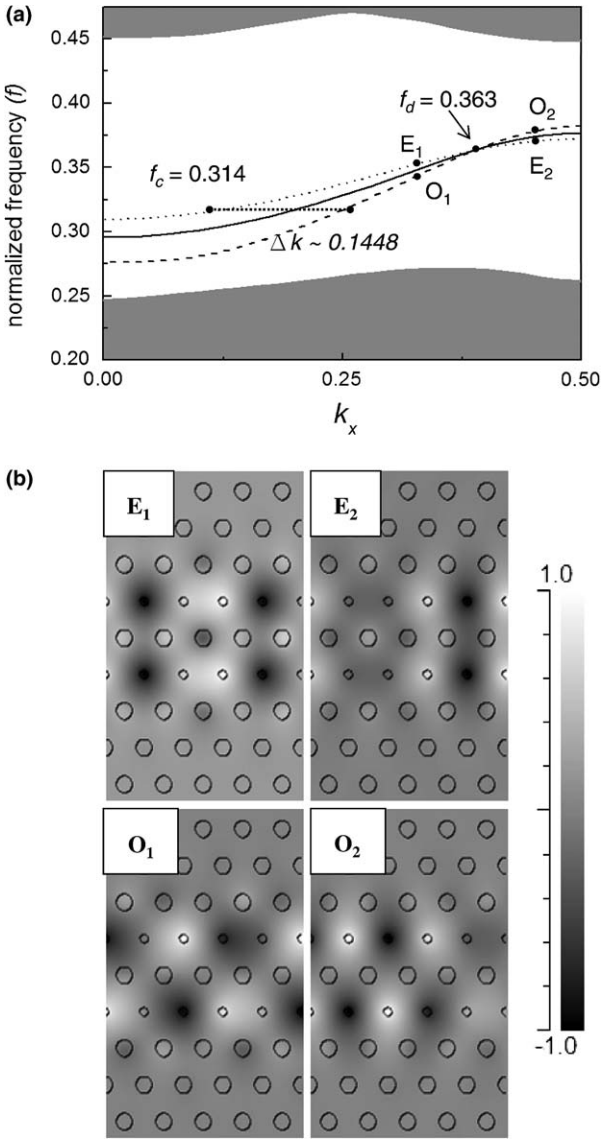

Fig. 4. (a) The dispersion curves of the guided mode of one reduced-rod PCW (solid curve) and coupled PCWs (dot curve and dash curve). These two curves of coupled PCWs cross at frequency of 0.363 (f_d) and the wavevector difference of the frequency at 0.314 (f_c) is 0.1448. (b) Electric eigenfield patterns derived by the PWE method at points E_1, E_2, O_1, and O_2, marked in (a).

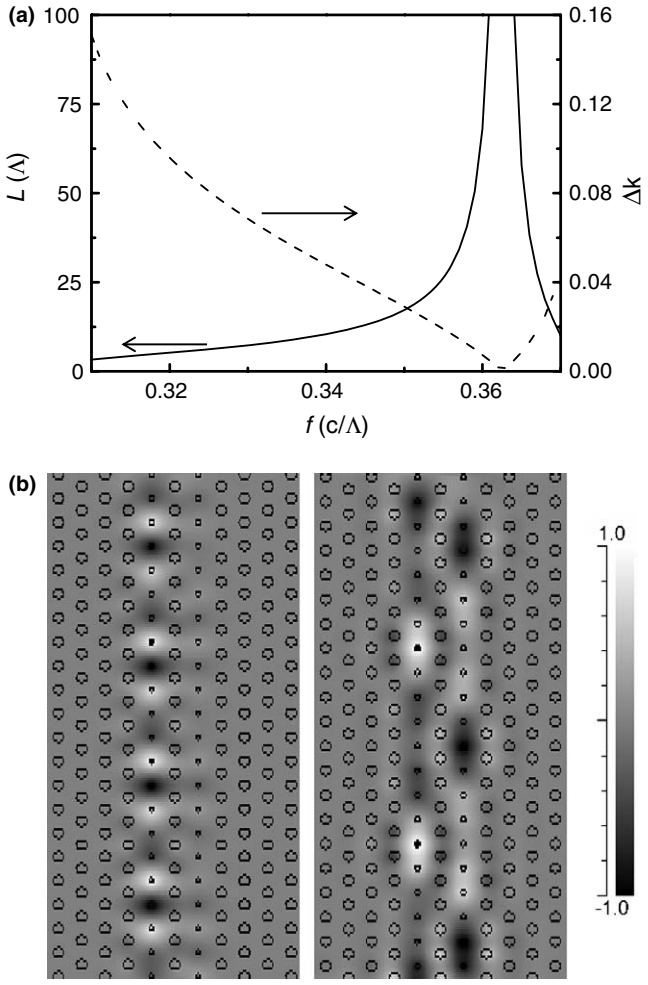

Fig. 5. (a) L and Δk as functions of frequency f, (b) the snapshots of the electric field evolution at f_d (left) and f_c (right) by the FDTD method.

time-domain (FDTD) method [22] (Fig. 5(b)). A Gaussian wave with a lateral width of $\sqrt{3}/2\Lambda$ is fed into the left PCW at f_d and f_c, respectively. The wave of f_d travels without transferring between the PCWs, indicating an infinite coupling length. On the other hand, the wave of f_c transfers periodically through the coupler with a coupling length about 4Λ. Both cases are in accordance with the prediction of the PWE.

Hence we checked the backward power in coupled PCWs by FDTD. The backward power at f_c traveling in the opposite direction in the right PCW as shown in Fig. 5(b) is -17 dB with respect to the forward power, while the backward power for coupled void-rod PCWs is -10 dB at the corresponding f_c (i.e., 0.361). The backward power is decreased by 7 dB due to introducing the reduced-rod defects. It supports our argument that the backward coupling is caused by the scattering with partition rods. Therefore, the reduced-rod PCW is a good candidate to construct a coupler with high coupling efficiency.

4. PCW coupler for Muxing and Demuxing

Taking advantage of the distinction between decoupling and coupling, we proposed a coupler to be utilized as an ultrashort dual-band Muxer/Demuxer. A one-by-two coupler composed of two reduced-rod PCWs is designed for multiplexing/demultiplexing (Muxing/Demuxing) of f_d and f_c (Fig. 6). The single port is denoted as *common*, and the dual ports as *direct* and *cross*, respectively. These PCWs are separated by five rows of rods. One PCW is truncated and the truncated end is bent toward the other PCW to have them coupled. The coupling region is 4Λ in length for the coupling of f_c. The Muxing and Demuxing simulated by the FDTD method are shown in Fig. 7. The waves of f_d and f_c are fed into the direct and cross ports, respectively, and the waves are successfully multiplexed

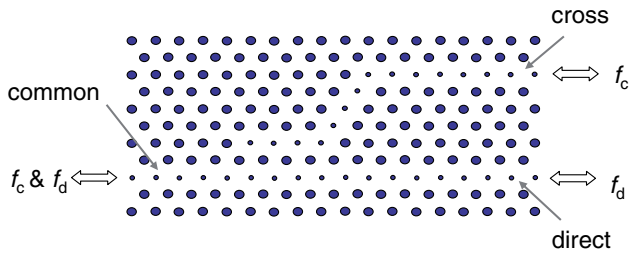

Fig. 6. The 1×2 reduced-rod PCW coupler for Muxing/Demuxing of f_c and f_d.

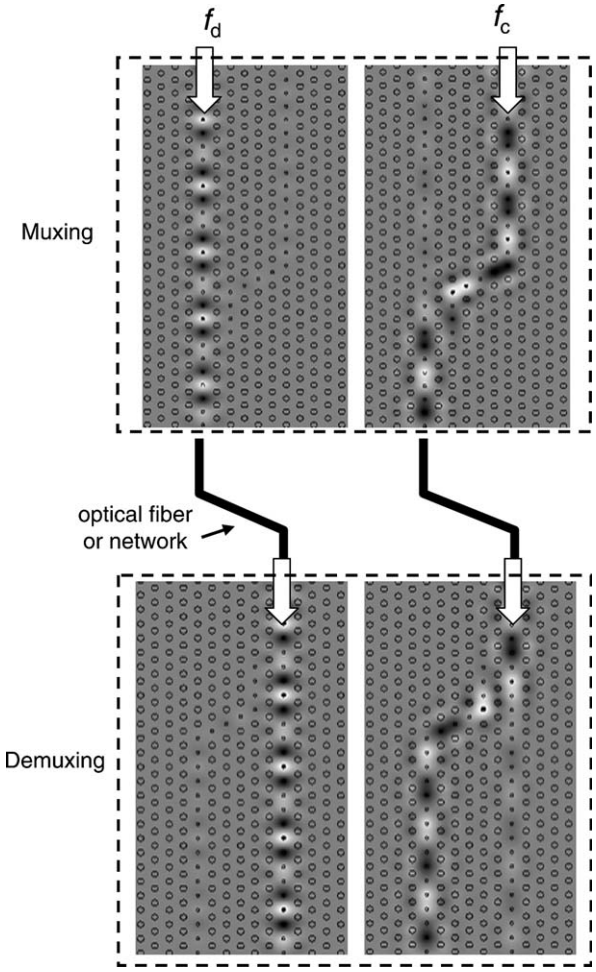

Fig. 7. Simulated Muxing and Demuxing with the coupler by the FDTD method. A dual-band bidirectional communication system can be built with the couplers at both ends, which is connected by an optical fiber or a network.

into the common port. As the waves are oppositely fed into the common port, they are demultiplexed into the direct and cross ports. Hence, the coupler can achieve decoupling at f_d and coupling at f_c bidirectionally with negligible backward coupling. That is a significant improvement for PCW couplers, since void-rod PCW couplers in our previous design [16] cannot achieve the bidirectional traffic.

A dual-band bidirectional system for duplex communication can be built by the couplers mentioned above. These two wavelength bands transmit at opposite directions. The system is composed of two identical couplers and one optical network. The optical network can be as simple as only a single fiber. The common ports of the couplers are connected by one fiber as shown in Fig. 7. The system has the dual ports on both ends; one direct (cross) port to transmit the wave of f_d (f_c), and the other direct (cross) port to receive the wave accordingly. The f_d and f_c can simultaneously transmit in the opposite directions. This system can be applied for the existing optical fiber communication, which utilizes the transparent windows of optical fibers at 1.3 and 1.5 μm wavelengths. The f_d serves for 1.3 μm and f_c for 1.5 μm as Λ is 0.48 μm. Therefore, the coupling region is only 1.92 μm in length, which is extremely small compared with other schemes, e.g., multiple layer thin films, fiber gratings, and other planar light wave circuit devices.

The transmission spectra of demultiplexing monitored at the *direct* and *cross* ports are shown in Fig. 8. At the *direct* port, the transmission power is completely suppressed at the coupling frequency around 0.321, and the power ratio of desired port to the other port reaches a maximum of 23 dB. The coupling frequency differs from f_c (=0.314) predicted by PWE. We suggest that the frequency discrepancy is due to the coupling length is not a multiple of Λ as our design. Since the coupling length is sensitive to frequency at this frequency range (see Fig. 5(a)), the power ratio varies rapidly with frequency. Hence, the operational bandwidth (>20 dB) is only 0.08%, corresponding to a bandwidth of 1.2 nm for the 1.5 μm wave. On the other hand, at the *cross* port, the transmission power is suppressed at the decoupling frequency 0.363, well correlative to f_d predicted by PWE, because the straight arm is nearly identical to the decoupled PCWs. The decoupling is effective as long as the coupling length is much larger than the coupling region, so it is insensitive to frequency. The operational bandwidth around f_d is 1.4%, covering a

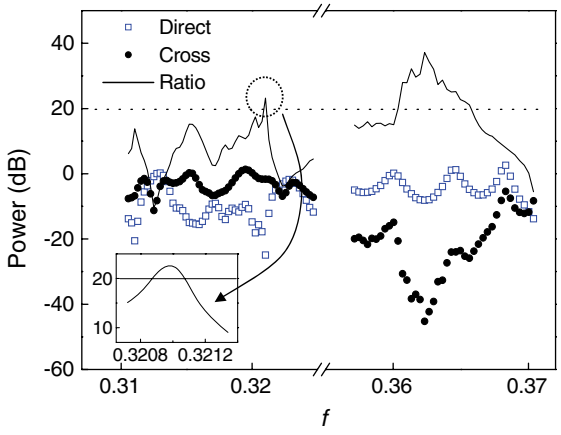

Fig. 8. The transmission spectra of demultiplexing at the direct and cross ports of the reduced-rod coupler. The power ratios are presented as the ratio of the powers at the desired port to the other. The ratio at the left side is the power at the cross port to the direct port, and the ratio at the right is reversed. Inset is the zoom-in at the peak over 20 dB.

18 nm window for the 1.3 μm wave. Therefore, such a dual-band bidirectional system requests a light source with high wavelength precision and stability at 1.5 μm. To use the system, the high-quality 1.5 μm light source should be installed at the server end and a low-quality 1.3 μm light source is installed at the user ends, to reduce the cost for light sources at the user ends.

The nature of wave localization in reduced-rod PCWs could be employed to improve the efficiency of transmission of other PCW devices, e.g., power splitters, other than Muxer/Demuxer. To design power splitters with zero reflections, additional specific defects are introduced by the concepts of rate matching [23] and perfect impedance matching [24]. However, to meet the matching conditions, one has to tune the positions and radius of these additional defects for the optimum transmission, consuming more time in computing. As the reduced-rod PCWs are employed to build the power splitters, the reflection should be suppressed due to the minor interaction with the adjacent rods.

Recently Chen et al., have experimentally demonstrated the possibility to build a directional coupler within the PhC of InAlGaAs rods [25]. Furthermore, the vertical confinement of the PCW can possibly be achieved as the PCW is sandwiched in antiresonant reflecting layers [26]. Hence, the ultrshort PCW coupler we proposed is feasible by current microfabricating technology. Moreover, such a three-dimensional dielectric complex can be effectively approximated with a 2D PhC presented above by the effective index method [27].

5. Conclusion

We describe the fundamental differences of the energy distributions in the void-rod and the reduced-rod PCWs. The energy is highly localized in the reduced rod. We suggest the energy dwells in the reduced rod and hops through the PCW. The backward coupling in the void-rod PCW couplers is caused by the energy scattering by the partition rods between the PCWs. The backward coupling is greatly suppressed in the reduced-rod PCW couplers due to the intense energy localization within the reduced rods. The PCW coupler with the reduced rods can achieve dual-band Muxing and Demuxing in use of coupling and decoupling. The coupling region for infrared wavelength is as short as 1.9 μm. This coupler is applicable to build a compact system for dual-band bidirectional optical communications.

Acknowledgments

We gratefully acknowledge partially financial support from the National Science Council (NSC) in Taiwan under Contract Nos. NSC-94-2112-M-009-035 and NSC-94-2112-M-092-004, and Tunghai Endowment Fund for Academic Advancement.

References

[1] T. Hashimoto, T. Kurosaki, M. Yanagisawa, Y. Suzuki, Y. Inoue, Y. Tohmori, K. Kato, Y. Yamada, N. Ishihara, K. Kato, J. Lightwave Technol. 18 (2000) 1541.
[2] E. Ghibaudo, J.-E. Broquin, P. Benech, Appl. Phys. Lett. 82 (2003) 1161.
[3] R.D. Meade, A. Devenyi, J.D. Joannopoulos, O.L. Alerhand, D.A. Smith, K. Kash, J. Appl. Phys. 75 (1994) 4753.
[4] V.N. Astratov, R.M. Stevenson, I.S. Culshaw, D.M. Whittaker, M.S. Skolnick, T.F. Krauss, R.M. De La Rue, Appl. Phys. Lett. 77 (2000) 178.
[5] M. Notomi, K. Yamada, A. Shinya, J. Takahashi, C. Takahashi, I. Yokohama, Phys. Rev. Lett. 87 (2001) 253902-1-4.
[6] A. Mekis, J.C. Chen, I. Kurland, S. Fan, P.R. Villeneuve, J.D. Joannopoulos, Phys. Rev. Lett. 77 (1996) 3787.
[7] A. Martinez, F. Cuesta, J. Marti, IEEE Photon. Technol. Lett. 15 (2003) 694.
[8] S. Kuchinsky, V.Y. Golyatin, A.Y. Kutikov, T.P. Pearsall, D. Nedeljkovic, IEEE J. Quantum Electron. 38 (2002) 1349.
[9] S. Boscolo, M. Midrio, C.G. Someda, IEEE J. Quantum Electron. 38 (2002) 47.
[10] A. Sharkawy, S. Shi, D.W. Prather, Opt. Exp. 10 (2002) 1048.
[11] A. Martinez, A. Griol, P. Sanchis, J. Marti, Opt. Lett. 28 (2003) 405.
[12] M. Qiu, B. Jaskorzynska, Appl. Phys. Lett. 83 (2003) 1074.
[13] I. Park, H.-S. Lee, H.-J. Kim, K.-M. Moon, S.-G. Lee, B.-H. O, S.-G. Park, E.-H. Lee, Opt. Exp. 12 (2004) 3599.
[14] M. Koshiba, J. Lightwave Technol. 19 (2001) 1970.
[15] A. Sharkawy, S. Shi, D.W. Prather, Appl. Opt. 40 (2001) 2247.
[16] F.S.-S. Chien, Y.-J. Hsu, W.-F. Hsieh, S.-C. Cheng, Opt. Exp. 12 (2004) 1119.
[17] T. Koponen, A. Huttunen, P. Törmä, J. Appl. Phys. 96 (2004) 4039.
[18] C.-W. Chang, S.-C. Cheng, W.-F. Hsieh, Opt. Commun. 242 (2004) 517.
[19] S.G. Johnson, J.D. Joannopoulos, Opt. Exp. 8 (2001) 173.
[20] T. Søndergaard, K.H. Dridi, Phys. Rev. B 61 (2000) 15688.
[21] S.-C. Cheng, W.-F. Hsieh, CWAB3-P74, IQEC and CLEO-Pacific Rim, July 11–15, 2005.
[22] A. Taflove, Computational Electrodynamics: The Finite-Difference Time-Domain Method, Artech, Norwood, MA, 1995.
[23] S. Fan, S.G. Johnson, J.D. Joannopoulos, C. Manolatou, H.A. Haus, J. Opt. Soc. Am. B 18 (2001) 162.
[24] S. Boscolo, M. Midrio, T.F. Krauss, Opt. Lett. 27 (2002) 1001.
[25] C.-C. Chen, C.-Y. Chen, W.-K. Wang, F.-H. Huang, C.-K. Lin, W.-Y. Chiu, Y.-J. Chan, Opt. Exp. 13 (2005) 38.
[26] M.A. Duguay, Y. Kukubun, T.L. Kock, L. Pfeiffer, Appl. Phys. Lett. 49 (1986) 13.
[27] M. Qiu, Appl. Phys. Lett. 81 (2002) 1163.